JIEMS
Journal of Industrial Engineering and Management Studies

Vol. 4, No. 2, 2017, pp. 19-34

DOI: 10.22116/JIEMS.2017.54603

www.jiems.icms.ac.ir

Performance of CCC-r control chart with variable sampling intervals

Mohammad Saber Fallah Nezhad[1,*], Yousof Shamstabar[1], Mohammad Mahdi Vali Siar[2]

Abstract

The CCC-r chart is developed based on cumulative count of a conforming (CCC) control chart that considers the cumulative number of items inspected until observing r nonconforming ones. Typically, the samples obtained from the process are analyzed through 100% inspection to exploit the CCC-r chart. However, considering the inspection cost and time would limit its implementation. In this paper, we investigate the performance of CCC-r chart with variable sampling interval (CCC-r_{VSI} chart). The efficiency of CCC-r_{VSI} chart is compared with fixed sampling interval (FSI) scheme of CCC-r chart (CCC-r_{FSI} chart) and CCC_{VSI} chart. The comparison results show that CCC-r_{VSI} chart is more efficient than the CCC_{VSI} chart in reducing the average time to signal (*ATS*) and also CCC-r_{VSI} chart performs better than CCC-r_{FSI} chart. In addition, some sensitivity analyses are performed to illustrate the effect of the input parameters on the performance of CCC-r_{VSI} chart.

Keywords: Attribute control chart; variable sampling interval; CCC-r chart; average time to signal

Received: July 2017-11

Revised: October 2017-06

Accepted: December 2017-06

1. Introduction

Attribute control chart is a tool for statistical process control (SPC) that is applied for increasing stability and improving quality through variability reduction in the production process. The cumulative count of conforming (CCC) control chart is a type of attribute control chart that is based on the cumulative number of conforming items between two consecutive nonconforming items and follows the geometric distribution (Calvin, 1983; Goh, 1987). It is useful for high-quality process like automated manufacturing systems. The extended state of CCC control chart is called CCC-r control chart which considers the cumulative count of conforming items until observing *r* non-conforming ones, and it is based on the negative binomial distribution (Ohta et al,2001; Kudo et al,2004). CCC chart is based

* Corresponding Author; Fallahnezhad@yazd.ac.ir
[1] Department of Industrial Engineering, Yazd University, Yazd, Iran.
[2] Department of Industrial Engineering, K.N. Toosi University of Technology, Tehran, Iran.

on the cumulative number of conforming items, but it makes the chart insensitive to process shifts relatively (Chen, 2014). Kuralmani et al. (2002) and Noorossana et al. (2007) proposed the conditional chart which detects the shifts of nonconforming fraction based on the current point and some of the previous ones in order to improve the performance of the CCC control chart .

Utilizing the scheme of variable sampling interval (VSI) that varies the next sampling interval between successive samples based on of the current point is another method for improving the sensitivity of the CCC chart (Liu et al. , 2006). The motivation of using variable sampling scheme is to decrease the cost of control chart implementation. Also, this chart detects the changes in nonconforming fraction more quickly than CCC chart with fixed sampling intervals (FSI). The length of sampling interval depends on the process condition in a VSI chart. If there are some alarms which show a change in the process, then a shorter sampling interval should be used and if there is no such signal, then a longer sampling interval will be used. If the current value of the control statistic is near to the target, then a longer sampling interval should be applied next, and a shorter sampling interval should be applied when the current value of the control statistic is near to but not outside the control limits.

A substantial number of researchers have considered VSI control chart in order to improve the performance of charts. $\bar{X}$ control chart with variable sampling interval was studied by some researchers (see for example, Reynolds et al., 1988; Reynolds and Arnold, 1989; Runger and Pignatiello Jr, 1991; Runger and Montgomery, 1993; Amin and Miller, 1993; Zhang et al., 2012; Lee et al., 2016). Aparisi and Haro (2001), Villalobos et al (2005) and Naderkhani and Makis (2016) considered a VSI multivariate Shewhart chart. Reynolds *et al.* (1990) and Luo and Wang, (2009) proposed the VSI CUSUM control chart to monitor the shift in the process mean. VSI EWMA charts have been investigated by some researchers (see for example, Shamma et al., 1991; Saccucci et al, 1992; Castagliolaet al, 2006; Castagliolaet et al, 2006). Vaughan(1992), Epprecht et al. (2003), Wu and Luo(2004), Zhou et al. (2016) and Lee and Khoo (2017) studied the VSI np control chart. Some studies considered CCC control chart with variable sampling interval (CCC_{VSI}). Liu et al. (2006) proposed cumulative count of conforming chart with variable sampling interval. They found that CCC_{VSI} chart is more effective than CCC_{FSI} chart. Chen et al. (2011) investigated CCC chart with variable sampling intervals and control limits ($CCC_{VSI/VCL}$ chart) and they concluded that the $CCC_{VSI/VCL}$ chart is more sensitive than both the CCC_{VSI} and CCC chart in detecting the process shift. Chen (2013) studied CCC chart with variable sampling interval for correlated samples ($GCCC_{VSI}$ chart). Their results demonstrated that using the $GCCC_{VSI}$ chart can enhance the speed of GCCC chart in detecting changes of the nonconforming fraction. Zhang et al. (2014) investigated the performance of CCC_{VSI} chart with estimated control limits. The performance of CCC_{VSI} chart with estimated parameters was compared with CCC_{FSI} based on two performance metrics, *ATS* and *SDATS*. They concluded that their proposed design is more efficient than CCC_{FSI} chart. Lee and Khoo (2015) proposed a combination of runs rules and variable sampling interval scheme for CCC chart. In this paper, we study CCC-r_{VSI} chart and compare its performance with the performance of CCC-r_{FSI} chart and CCC_{VSI} proposed by Liu et al. (2006). The rest of the paper is organized as follows. In section 2, the CCC-r_{VSI} Chart has been described. In section 3, the comparison study between the CCC-r_{VSI} chart and the CCC-r_{FSI} chart and CCC_{VSI} chart is conducted and the effect of parameters is elaborated using sensitivity analysis. In section 4, a practical case study for the implementation of the CCC-r_{VSI} chart is described. Finally, the paper is concluded.

2. Description of the CCC-r_{VSI} Chart

2.1. Notations

p_0	the in-control nonconforming fraction,
p_1	the out-of-control nonconforming fraction,
α	the true probability of false alarm,
X_i	the cumulative count of items inspected between the $(i-1)_{th}$ nonconforming item and the i_{th} nonconforming item (including the last nonconforming item),
N	the number of sampling interval lengths for the CCC-r_{VSI} chart,
d_j	$j = 1,2,\ldots,n$. Sampling interval lengths of the CCC-r_{VSI} chart, , i.e., the time between inspections of two consecutive items ($d_n < d_{n-1} < \ldots < d_2 < d_1$)
d	the sampling interval length of the CCC-r_{FSI} chart,
IL	the limits in the CCC-r_{VSI} chart which divide the region between UCL and LCL into n sub-regions $I_1; I_2; \ldots ; I_n$ ($IL_{n-1} < IL_{n-2} < \ldots < IL_1$),
L_i	the sampling interval length which is used to obtain X_i,
ARL	the average run length,
ATS	the average time to signal,
ATS_V	the in-control ATS of the CCC-r_{VSI} chart,
ATS_F	the in-control ATS of the CCC-r_{FSI} chart,
ATS'_V	The out-of-control ATS of the CCC-r_{VSI} chart,
ATS'_F	the out-of-control ATS of the CCC-r_{FSI} chart,
I	improvement factor, defined as $I = ATS'_V / ATS'_F$,
q_j	the probability that point X_i falls within the region I_j when the process nonconforming fraction is p_0 ,
q'_j	the probability that point X_i falls within the region I_j when the process nonconforming fraction is p_1 ,

2.2. CCC-r_{VSI} control chart

As mentioned before, The CCC–r charts are based on the cumulative count of conforming items until detecting *r* nonconforming item. Assume a process with nonconforming fraction of *p* and let *X* denote the cumulative count of items inspected until the detection of the r_{th} nonconforming item, then *X* follows the negative binomial distribution with parameters (*r*, *p)* and the probability mass function of *X* as is following,

$$f(x) = \binom{x-1}{r-1}(1-p)^{x-r} p^r, x = r, r+1, \ldots, \infty \quad (1)$$

The cumulative distribution function of *X* as is follows,

$$F(x) = \sum_{i=r}^{x} \binom{i-1}{r-1} (1-p)^{i-r} p^r \qquad (2)$$

If the acceptable risk of false alarm is *α*, then the upper control limit, *UCL* the central control limit, *CL* and the lower control limit, *LCL* of the CCC-r control charts are as following(Xie et al, 2012):

$$\sum_{i=r}^{UCL-1} \binom{i-1}{r-1} (1-p_0)^{i-r} p_0{}^r = 1-\alpha/2 \qquad (3)$$

$$\sum_{i=r}^{CL} \binom{i-1}{r-1} (1-p_0)^{i-r} p_0{}^r = 0.5 \qquad (4)$$

$$\sum_{i=r}^{LCL} \binom{i-1}{r-1} (1-p_0)^{i-r} p_0{}^r = \alpha/2 \qquad (5)$$

When a point falls outside the control limits, then the process is considered to be out of control. It is necessary to mention that if a plotted point of the CCC−r chart is above the upper control limit, then we have an improvement in the process. On the other hand, a point below the lower control limit is a signal of process deterioration.

The *ARL* (average run length) is the average number of points plotted until receiving an out-of-control signal. For the CCC−r charts, *ARL* can be calculated from Eq. (6), with specified values of nonconforming fraction $p \neq p_0$ and $p = p_0$ for out of control and in control situations respectively.

$$ARL = \frac{1}{1 - \sum_{LCL}^{UCL} \binom{i-1}{r-1} p^r (1-p)^{i-r}} \qquad (6)$$

ANI is the average number of items inspected until a nonconforming signal occurs, that can be calculated for CCC-r_{FSI} and CCC-r_{VSI} chart by using the following equation:

$$ANI = \frac{r}{p} ARL \qquad (7)$$

When the CCC-r_{VSI} chart is applied, then a finite number of interval lengths $d_1, d_2, \ldots, d_n (d_1 > d_2 > \ldots > d_n)$ are used. These interval lengths should be determined based on the practical conditions of manufacturing processes. The interval limits $IL_1, IL_2, \ldots, IL_n$ are designed in the CCC-r_{VSI} chart, so that the region between *UCL* and *LCL* is divided into n sub-regions $I_1, I_2, \ldots, I_n$, corresponding to the n different intervals. Thus following framework is used for sampling from the process,

$$L_i = \begin{cases} d_1, X_{i-1} \in I_1 = (IL_1, UCL) \\ d_2, X_{i-1} \in I_2 = (IL_2, IL_1) \\ . \\ . \\ . \\ d_n, X_{i-1} \in I_n = (LCL, IL_n) \end{cases} \quad (8)$$

The sampling interval length, L_i that is used for inspection between the (i-1) th nonconforming item and the ith nonconforming item depends on the value of X_{i-1}. The interval limits $IL_1, IL_2, \ldots, IL_{n-1}$ can be computed as follows (F^{-1} is inverse function of the negative binomial distribution with parameters *r* and p_0):

$$\begin{cases} IL_1 = F^{-1}(1 - q_1 - \frac{\alpha}{2}) \\ IL_2 = F^{-1}(1 - q_1 - q_2 - \frac{\alpha}{2}) \\ . \\ . \\ . \\ IL_{n-1} = F^{-1}(1 - q_1 - q_2 - \ldots - q_n - \frac{\alpha}{2}) \end{cases} \quad (9)$$

This scheme continues until the *IL* values fall between *UCL* and *LCL*. It can be elaborated as follows:

$$LCL < IL_{n-1} < IL_{n-2} < \ldots < IL_2 < IL_1 < UCL \quad (10)$$

$$IL_1 = F^{-1}(1 - q_1 - \frac{\alpha}{2}) < UCL, IL_{n-1} = F^{-1}(1 - q_1 - q_2 - \ldots - q_n - \frac{\alpha}{2}) > LCL \quad (11)$$

For example, when *n*=4; then four different intervals are applied. For implementing the CCC-r_{VSI} scheme, control limits IL_1, IL_2 and IL_3 are designed between *UCL* and *LCL*, so that the region (*LCL*, *UCL*) is divided into four sub-regions.

Therefore, *ATS* can be calculated based on the following equations:

$$ATS_F = ANI \times d = ARL \times \frac{r}{p} \times d \tag{12}$$

$$ATS_V = ARL \times \frac{r}{p} \times \frac{d_1 q_1 + d_2 q_2 + ... + d_n q_n}{q_1 + q_2 + ... + q_n} \tag{13}$$

3. Performance comparisons between the CCC-r$_{VSI}$ and the CCC-r$_{FSI}$ chart

In order to evaluate the efficiency of the CCC-r$_{VSI}$ chart, its performance is compared with the CCC-r$_{FSI}$ chart in this section. Note that the fixed values of nonconforming fraction p_0 and acceptable risk of false alarm α are assumed for both the CCC$_{FSI}$ and the CCC$_{VSI}$ chart so that these charts have the same *ANI* value. In order to compare their *ATS* values, we opt appropriate design parameters for the CCC-r$_{VSI}$ and the CCC-r$_{FSI}$ chart so that the equation $ATS_F=ATS_V$ is satisfied at the in control state. Therefore the CCC$_{VSI}$ chart will be matched to the corresponding CCC-r$_{FSI}$ chart when $p=p_0$ and both of them have the same in-control *ATS*. On the other hand, when the process nonconforming fraction changes to $p_1(> \mathrm{p}_0)$, the values of ATS'_F and ATS'_V should be compared. The control chart with smaller out-of-control ATS' can detect the shift of nonconforming fraction more quickly.

Let $ATS_F = ATS_V$, thus,

$$d = \frac{d_1 q_1 + d_2 q_2 + ... + d_n q_n}{q_1 + q_2 + ... + q_n} = \frac{d_1 q_1 + d_2 q_2 + ... + d_n q_n}{1-\alpha} \tag{14}$$

Thus, the sampling interval length of the CCC-r$_{FSI}$ chart is adjusted to be equal 1(d =1), then by selecting appropriate value values of $(d_1, d_2, ..., d_n)$ and $(q_1, q_2, ..., q_n)$ that satisfy Eq. (14), we can obtain the matched CCC-r$_{VSI}$ and CCC-r$_{FSI}$ chart that have the same in-control value of *ATS*. Then, when the nonconforming fraction shifts to p_1, the performance of the CCC-r$_{VSI}$ chart can be analyzed by computing the value of *I*, that is the ratio of out-of-control *ATS* of the CCC-r$_{VSI}$ and the CCC-r$_{FSI}$ chart:

$$I = \frac{ATS'_V}{ATS'_F} = \frac{d_1 q'_1 + d_2 q'_2 + ... + d_n q'_n}{q'_1 + q'_2 + ... + q'_n} \tag{15}$$

When I is less than 1.00, the ATS'_V is less than ATS'_F . It indicates that the CCC-r$_{VSI}$ chart performs better than the CCC-r$_{FSI}$ chart. Thus the ratio *I* is the improvement factor. The smaller values of the improvement factor denote an improvement in the performance of the CCC-r$_{VSI}$ chart.

The values of q'_j can be calculated using the following equations:

$$\begin{cases} q'_1 = \sum_{x=IL_1+1}^{UCL-1} \binom{x-1}{r-1} p_1^{\,r} (1-p_1)^{x-r} \\ q'_2 = \sum_{x=IL_2+1}^{IL_1} \binom{x-1}{r-1} p_1^{\,r} (1-p_1)^{x-r} \\ . \\ . \\ . \\ q'_{n-1} = \sum_{x=IL_{n-1}+1}^{IL_{n-2}} \binom{x-1}{r-1} p_1^{\,r} (1-p_1)^{x-r} \\ q'_n = \sum_{x=LCL+1}^{IL_{n-1}} \binom{x-1}{r-1} p_1^{\,r} (1-p_1)^{x-r} \end{cases} \quad (16)$$

3.1. Application of CCC-r charts with variable sampling intervals

We now study the behavior of CCC-r_{VSI} chart based on equal probabilities for each interval:

$$q_1 = q_2 = ... = q_n = \frac{1-\alpha}{n} \quad (17)$$

By using Eq. (14) and substituting $d = 1$, we have,

$$1-\alpha = d_1 q_1 + d_2 q_2 + ... + d_n q_n = \frac{1-\alpha}{n}(d_1 + d_2 + ... + d_n)$$

Thus following equation is obtained,

$$d_1 + d_2 + ... + d_n = n \quad (18)$$

In this paper, we used data of Liu et.al (2006) for comparison study. They have assumed $\alpha = 0.0027, p_0 = 0.0005$ and sampling interval lengths $(d_1, d_2, ..., d_n)$ with the fixed value of $d = 1$ can be chosen as follows:

$$n = 2, d_1 = 1.9, d_2 = 0.1; n = 3, d_1 = 1.9, d_2 = 1, d_3 = 0.1; \mathrm{n} = 4, \mathrm{d}_1 = 1.9, d_2 = 1.2, d_3 = 0.8, d_4 = 0.1;$$
$$\mathrm{n} = 5, \mathrm{d}_1 = 1.9, d_2 = 1.5, d_3 = 1, d_4 = 0.5, \mathrm{d}_5 = 0.1; ...$$

Based on the equations 10 and 11 for each value of the parameter r, possible values for the number of intervals (n) will be obtained. For example in the case CCC_{VSI} (r=1), when n=1538, the value of IL_{1537} is equal to LCL according to the equation 11. Thus, this scheme is only possible for the cases n=2, 3,…, 1537. This analysis is denoted in Table 1. Also, the possible value of n can be obtained for other values of r based on constraint (10) and (11).

Table 1. Possible number of intervals (*n*) for implementing CCC_{VSI} control chart

n	IL_1, IL_{n-1}	result
2	$LCL = 3 < IL_1 = 1385 < UCL = 13426$	possible
3	$IL_1 = 2193 < UCL, IL_2 = 812 > LCL$	possible
.	.	.
.	.	.
.	.	.
1537	$IL_1 = 12427 < UCL, IL_{1536} = 4 > LCL$	possible
1538	$IL_1 = 12427 < UCL, IL_{1537} = 3 = LCL$	impossible
1539	$IL_1 = 12428 < UCL, IL_{1538} = 3 = LCL$	impossible

3.2. Improvement factors for different CCC-r control chart based on the number of intervals

In this subsection, by fixing n and based on the assumed parameters in the previous subsection and possible values of r, it is observed that when nonconforming fraction, p_1 increases then the improvement factor decreases which demonstrates better performance of CCC-r_{VSI} compared to CCC-r_{FSI}. The results are denoted in Table 2. Also when the parameter r increases, then improvement factor decreases which denotes an improvement in the performance of CCC-r_{VSI} chart. As can be seen in Table 2, (for all values of nonconforming fraction and the parameter *r*) the values of *I* are less than 1, thus the performance of CCC-r_{VSI} chart is always better than CCC-r_{FSI} chart.

Table 2. Improvement factors with fixed number of intervals (*n*=3)

***n*=3**	**improvement factor, *I***			
p_1/p_0	***r*=1**	***r*=2**	***r*=3**	***r*=4**
1	1.000	1.000	1.000	1.000
1.1	0.945	0.917	0.897	0.880
1.2	0.894	0.842	0.802	0.770
1.3	0.848	0.772	0.717	0.673
1.4	0.804	0.709	0.641	0.587
1.5	0.764	0.651	0.573	0.512
1.6	0.726	0.599	0.512	0.448
1.7	0.691	0.551	0.459	0.392
1.8	0.659	0.509	0.413	0.345
1.9	0.629	0.470	0.372	0.305
2	0.601	0.435	0.336	0.271

3.3. Improvement factors for different numbers of sampling intervals

As shown in Table 3, when *n*=2 and the ratio $\frac{p_1}{p_0}$ equals 2, then I = 0.278. It indicates that the CCC-r$_{VSI}$ chart has the best performance in the case *n*=2 among the other values. Also, with increasing the ratio $\frac{p_1}{p_0}$ the value of *I* decreases.

Table 3. Improvement factors *I* for different values of number of intervals

***r*=3**	**Improvement factor, *I***			
p₁/p₀	***n*=2**	***n*=3**	***n*=4**	***n*=5**
1	1.000	1.000	1.000	1.000
1.1	0.886	0.897	0.905	0.904
1.2	0.782	0.802	0.819	0.817
1.3	0.687	0.717	0.741	0.738
1.4	0.602	0.641	0.671	0.667
1.5	0.527	0.573	0.608	0.604
1.6	0.462	0.512	0.552	0.547
1.7	0.405	0.459	0.502	0.497
1.8	0.356	0.413	0.458	0.453
1.9	0.314	0.372	0.418	0.413
2	0.278	0.336	0.383	0.378

3.4. Improvement factors based on different lengths of sampling interval

In this subsection, the number of sampling intervals has been fixed (*n*=2) and the length of sampling intervals has been changed in order to analyze how the performance of CCC$_{VSI}$ charts varies. Four different cases of (d_1, d_2) are chosen and without changing the other parameters, their corresponding improvement factors, *I* are determined.

As can be seen in Table 4, when the ratio $\frac{p_1}{p_0}$ increases, then the improvement factors, *I* decreases and the performance of CCC-r$_{VSI}$ charts improves compared to the CCC-r$_{FSI}$ charts. Besides, it demonstrates that applying larger values for the differences of interval lengths, (d_1 - d_2) leads to smaller values of the improvement factor and consequently better performance of CCC-r$_{VSI}$ charts.

Table 4. Improvement factors *I* with different values of sampling interval lengths (d_1, d_2) for *n*=2

		improvement factor, *I*				
r		(d_1,d_2)				
	p_1/p_0	**FSI(1,1)**	**(1.9,0.1)**	**(1.7,0.3)**	**(1.5,0.5)**	**(1.2,0.8)**
1	1	1.000	1.000	1.000	1.000	1.000
	1.1	1.000	0.940	0.953	0.967	0.987
	1.2	1.000	0.884	0.910	0.936	0.974
	1.3	1.000	0.832	0.869	0.907	0.963
	1.4	1.000	0.783	0.831	0.880	0.952
	1.5	1.000	0.737	0.796	0.854	0.942
	1.6	1.000	0.695	0.763	0.830	0.932
	1.7	1.000	0.655	0.732	0.808	0.923
	1.8	1.000	0.618	0.703	0.788	0.915
	1.9	1.000	0.583	0.676	0.769	0.907
	2	1.000	0.551	0.651	0.751	0.900
2	1	1.000	1.000	1.000	1.000	1.000
	1.1	1.000	0.909	0.929	0.950	0.980
	1.2	1.000	0.825	0.864	0.903	0.961
	1.3	1.000	0.747	0.804	0.860	0.944
	1.4	1.000	0.677	0.748	0.820	0.928
	1.5	1.000	0.612	0.698	0.784	0.914
	1.6	1.000	0.554	0.653	0.752	0.901
	1.7	1.000	0.501	0.612	0.723	0.889
	1.8	1.000	0.454	0.576	0.697	0.879
	1.9	1.000	0.412	0.543	0.673	0.869
	2	1.000	0.375	0.514	0.653	0.861
3	1	1.000	1.000	1.000	1.000	1.000
	1.1	1.000	0.886	0.912	0.937	0.975
	1.2	1.000	0.782	0.830	0.879	0.952
	1.3	1.000	0.687	0.757	0.826	0.930
	1.4	1.000	0.602	0.691	0.779	0.912
	1.5	1.000	0.527	0.632	0.737	0.895
	1.6	1.000	0.462	0.581	0.701	0.880
	1.7	1.000	0.405	0.537	0.669	0.868
	1.8	1.000	0.356	0.499	0.642	0.857
	1.9	1.000	0.314	0.467	0.619	0.848
	2	1.000	0.278	0.439	0.599	0.840

3.5. Improvement factors for different probability allocations

The overall performance of CCC_{VSI} is analyzed based on the equal in-control probability allocations. Thus, in order to investigate the overall performance of CCC_{VSI} chart when the condition $q_1=q_2=\cdots=q_n$ is not satisfied, we fix n=2 and d_1=1.9 and only change the values of in control probability q_1 as suggested by Liu et al. (2006). It should be noted that:

$q_1+q_2=1-\alpha$. Thus, d_2 can
be calculated as follows based on Eq. (19).

$$d_2 = \frac{1-\alpha-d_1q_1}{q_2} > 0 \qquad (19)$$

Thus, q_1 should satisfy the inequality $q_1 < (1-\alpha)/d_1$ for fixed value of d_1.

The results in Table 5, indicate that when (q_2-q_1) decreases, then the improvement factor, *I* decreases and the performance of CCC-r$_{VSI}$ charts improves.

Table 5. Improvement factors *I* with different probability allocation for CCC-r chart with *n*=2

			Improvement factors *I* with different probability allocation				
		(q_1,q_2)	**(0.10,0.8973)**	**(0.2,0.7973)**	**(0.3,0.6973)**	**(0.4,0.5973)**	**(0.49865,0.49865)**
r	***p_1/p_0***	***(d_1,d_2)***	**(1.9,0.8997)**	**(1.9,0.7742)**	**(1.9,0.6128)**	**(1.9,0.3973)**	**(1.9, 0.1)**
	1		1.000	1.000	1.000	1.000	1.000
	1.1		0.98	0.967	0.957	0.948	0.94
	1.2		0.964	0.939	0.918	0.9	0.884
	1.3		0.951	0.914	0.884	0.856	0.832
	1.4		0.94	0.894	0.853	0.816	0.783
1	1.5		0.932	0.876	0.826	0.78	0.737
	1.6		0.925	0.861	0.802	0.747	0.695
	1.7		0.92	0.848	0.781	0.716	0.655
	1.8		0.916	0.837	0.762	0.688	0.618
	1.9		0.913	0.828	0.745	0.663	0.583
	2		0.91	0.82	0.73	0.64	0.551
	1		1.000	1.000	1.000	1.000	1.000
	1.1		0.974	0.955	0.938	0.923	0.909
	1.2		0.954	0.918	0.885	0.855	0.825
	1.3		0.939	0.888	0.84	0.793	0.747
	1.4		0.928	0.864	0.801	0.739	0.677
2	1.5		0.92	0.844	0.769	0.692	0.612
	1.6		0.914	0.829	0.742	0.65	0.554
	1.7		0.91	0.817	0.719	0.614	0.501
	1.8		0.907	0.808	0.7	0.582	0.454
	1.9		0.905	0.8	0.684	0.555	0.412
	2		0.903	0.794	0.671	0.532	0.375
	1		1.000	1.000	1.000	1.000	1.000
	1.1		0.969	0.946	0.925	0.906	0.886
	1.2		0.947	0.903	0.862	0.822	0.782
	1.3		0.932	0.871	0.811	0.75	0.687
	1.4		0.921	0.845	0.768	0.688	0.602
3	1.5		0.914	0.826	0.734	0.635	0.527
	1.6		0.909	0.812	0.707	0.591	0.462
	1.7		0.906	0.802	0.686	0.554	0.405
	1.8		0.904	0.794	0.669	0.524	0.356
	1.9		0.902	0.789	0.656	0.499	0.314
	2		0.901	0.784	0.645	0.479	0.278

4. Design of a CCC-r$_{VSI}$ chart

In designing a CCC-r$_{VSI}$ chart, the nonconforming fraction p_0, acceptable false alarm probability α, parameter r and the number of intervals and their lengths in the CCC-r$_{VSI}$ chart should be determined. According to the methodologies elaborated so for, the design procedure is suggested as follows.

Step 1: Determine the control limits based on fixed false alarm probability α .

Step 2: Select the number of sampling intervals.

Step 3: Select the method of probability allocation.

Step 4: Determine the length of sampling intervals ($d_1, d_2, \dots, d_n$).

Step 5: Evaluate the efficiency of CCC-r$_{VSI}$ charts: All of the design parameters of the CCC-r$_{VSI}$ chart can be determined by implementing the above four steps. When the shifted nonconforming fraction is p_1 , then the probability allocation (q_1', q_2') can be calculated using Eq. (16), then the improvement factor I can be computed using Eq. (15), that can be used to evaluate the efficiency of the CCC-r$_{VSI}$ chart.

To illustrate the design procedure of a CCC$_{VSI}$ chart, we suppose that $p_0 = 0.0005$, $\alpha = 0.0027$, n=2, (d_1,d_2)=(1.9,0.1). The data of Table 6 show the input defect sequence. As can be seen in Fig. 1, CCC-r$_{VSI}$ charts are drawn for different values of parameter r. It is concluded that no signal is observed.

Table 6. A set of data follow geometric distribution with nonconforming rate p_0 = 0.0005

Defect sequence	CCC	Defect sequence	CCC	Defect sequence	CCC	Defect sequence	CCC	Defect sequence	CCC
1	102	11	970	21	5696	31	8361	41	353
2	2928	12	466	22	2082	32	583	42	7858
3	998	13	162	23	413	33	1618	43	767
4	1442	14	606	24	9235	34	141	44	1937
5	230	15	3470	25	3947	35	1526	45	368
6	543	16	1803	26	3190	36	1741	46	1374
7	1568	17	133	27	3230	37	333	47	686
8	7977	18	173	28	1008	38	1287	48	1692
9	393	19	1781	29	2601	39	3191	49	2376
10	1620	20	224	30	3229	40	794	50	3324

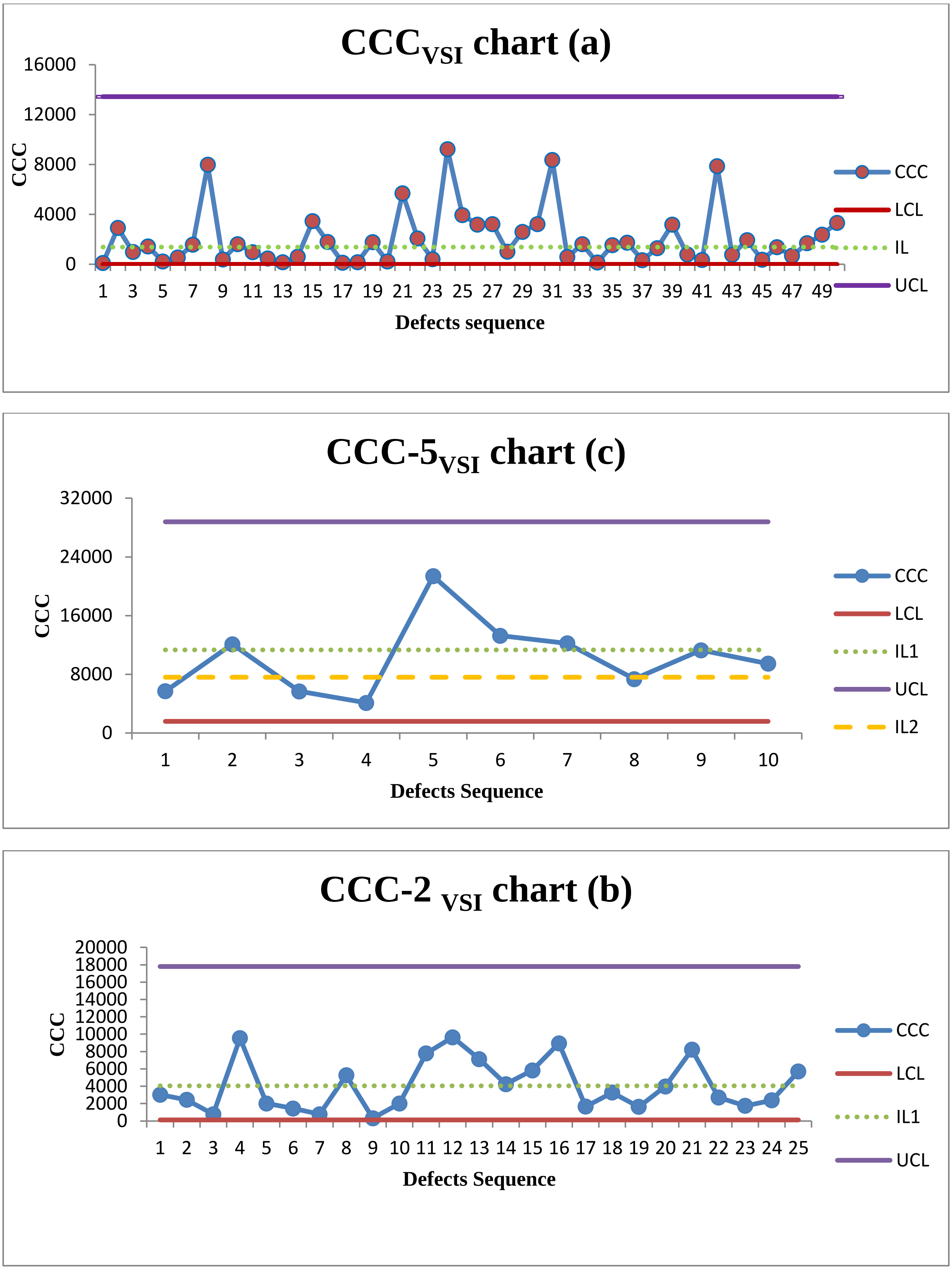

Figure 1. An example of the CCC$_{VSI}$ chart(a), CCC-2$_{VSI}$ chart(b) and CCC-5$_{VSI}$ chart(c) with *n*=2.

5. Conclusion

In this paper, we have proposed the CCC-r_{VSI} control chart for high quality processes. The CCC-r chart is an improved form of CCC charts. Also, we compared CCC-r_{VSI} chart with CCC_{VSI} chart that has been studied by Liu et al. (2006). The results of this study have demonstrated that always CCC_{VSI} chart is more efficient than CCC_{FSI} chart and also CCC-r_{VSI} charts perform better than CCC_{VSI} chart. It is denoted that the efficiency of CCC-r_{VSI} chart can be enhanced by increasing the difference between interval lengths. The results show that when probability allocation is equal, then the performance of CCC-r_{VSI} chart becomes better. In CCC-r_{VSI} chart, if parameter r increases, then the improvement factor of CCC-r_{VSI} chart will decrease. Thus, CCC-r_{VSI} chart can detect the nonconforming fraction shift faster than CCC_{VSI} chart. Also, we compared CCC-r_{VSI} chart with CCC-r_{FSI} chart and concluded that CCC-r_{VSI} chart is always more efficient than CCC-r_{FSI} chart.

References

Amin, R. W., and Miller, R. W., (1993). "A robustness study of X charts with variable sampling intervals", *Journal of Quality Technology*, Vol. 25, pp. 36-36.

Aparisi, F., and Haro, C. L., (2001). "Hotelling's T2 control chart with variable sampling intervals", *International Journal of Production Research*, Vol. 39, No. 14, pp. 3127-3140.

Calvin, T., (1983). "Quality Control Techniques for" Zero Defects", *IEEE Transactions on Components, Hybrids, and Manufacturing Technology*, Vol. 6, No. 3, pp. 323-328.

Castagliola, P., Celano, G., and Fichera, S., (2006). "Evaluation of the statistical performance of a variable sampling interval R EWMA control chart", *Quality Technology & Quantitative Management*, Vol. 3, No. 3, pp. 307-323.

Castagliola, P., Celano, G., Fichera, S., and Giuffrida, F., (2006). "A variable sampling interval S2-EWMA control chart for monitoring the process variance", *International Journal of Technology Management*, Vol. 37, pp. 125-146.

Chen, Y.-K., (2013). "Cumulative conformance count charts with variable sampling intervals for correlated samples", *Computers & Industrial Engineering*, Vol. 64, No. 1, pp. 302-308.

Chen, Y. K., Chen, C. Y., & Chiou, K. C., (2011). "Cumulative conformance count chart with variable sampling intervals and control limits", *Applied stochastic models in business and industry*, Vol. 27, No. 4, pp. 410-420.

Epprecht, E. K., Costa, A. F., and Mendes, F. C., (2003). "Adaptive control charts for attributes", *IIE Transactions*, Vol. 35, No. 6, pp. 567-582.

Goh, T., 1987. A control chart for very high yield processes. Quality Assurance, 13(1), 18-22.

Kudo, K., Ohta, H., and Kusukawa, E., (2004). "Economic Design of A Dynamic CCC–r Chart for High-Yield Processes", *Economic Quality Control*, Vol. 19, No. 1, pp. 7-21.

Kuralmani, V., Xie, M., Goh, T., and Gan, F., (2002). "A conditional decision procedure for high yield processes", *IIE Transactions*, Vol. 34, No. 12, pp. 1021-1030.

Lee, M. H., and Khoo, M. B., (2015). "Variable sampling interval cumulative count of conforming chart with runs rules", *Communications in statistics-simulation and computation*, Vol. 44, No. 9, pp. 2410-2430.

Lee, M. H., and Khoo, M. B., (2017). "Combined Double Sampling and Variable Sampling Interval np Chart", Communications in Statistics-Theory and Methods (accepted manuscript).

Lee, T.-H., Hong, S.-H., Kwon, H.-M., and Lee, M., (2016). "Economic Statistical Design of Variable Sampling Interval X Control Chart Based on Surrogate Variable Using Genetic Algorithms", *Management and Production Engineering Review*, Vol. 7, No. 4, pp. 54-64.

Liu, J., Xie, M., Goh, T., Liu, Q., and Yang, Z., (2006). "Cumulative count of conforming chart with variable sampling intervals", *International Journal of Production Economics*, Vol. 101, No. 2, pp. 286-297.

Luo, Y., Li, Z., and Wang, Z., (2009). "Adaptive CUSUM control chart with variable sampling intervals", *Computational Statistics & Data Analysis*, Vol. 53, No. 7, pp. 2693-2701.

Naderkhani, F., and Makis, V., (2016). "Economic design of multivariate Bayesian control chart with two sampling intervals", *International Journal of Production Economics*, Vol. 174, pp. 29-42.

Noorossana, R., Saghaei, A., Paynabar, K., and Samimi, Y., (2007). "On the conditional decision procedure for high yield processes", *Computers & Industrial Engineering*, Vol. 53, No. 3, pp. 469-477.

Ohta, H., Kusukawa, E., and Rahim, A., (2001). "A CCC-r chart for high-yield processes", *Quality and Reliability Engineering International*, Vol. 17, No. 6, pp. 439-446.

Reynolds Jr, M. R., and Arnold, J. C., (1989). "Optimal one-sided Shewhart control charts with variable sampling intervals", *Sequential Analysis*, Vol. 8, No. 1, pp. 51-77.

Reynolds, M. R., Amin, R. W., and Arnold, J. C., (1990). "CUSUM charts with variable sampling intervals", *Technometrics*, Vol. 32, No. 4, pp. 371-384.

Reynolds, M. R., Amin, R. W., Arnold, J. C., and Nachlas, J. A., (1988). "Charts with variable sampling intervals", *Technometrics*, Vol. 30, No. 2, pp. 181-192.

Runger, G. C., and Montgomery, D. C., (1993). "Adaptive sampling enhancements for Shewhart control charts", *IIE Transactions*, Vol. 25, No. 3, pp. 41-51.

Runger, G. C., and Pignatiello Jr, J. J., (1991). "Adaptive sampling for process control", *Journal of Quality Technology*, Vol. 23, No. 2, pp. 135-155.

Saccucci, M. S., Amin, R. W., and Lucas, J. M., (1992). "Exponentially weighted moving average control schemes with variable sampling intervals", *Communications in Statistics-simulation and Computation*, Vol. 21, No. 3, pp. 627-657.

Shamma, S. E., Amin, R. W., and Shamma, A. K., (1991). "A double exponentially weighted moving average control procedure with variable sampling intervals", *Communications in Statistics-simulation and Computation*, Vol. 20, pp. 511-528.

Vaughan, T. S., (1992). "Variable sampling interval np process control chart", *Communications in Statistics-Theory and Methods*, Vol. 22, No. 1, pp. 147-167.

Villalobos, J. R., Muñoz, L., and Gutierrez, M. A., (2005). "Using fixed and adaptive multivariate SPC charts for online SMD assembly monitoring", *International Journal of Production Economics*, Vol. 95, No. 1, pp. 109-121.

Wu, Z., and Luo, H., (2004). "Optimal design of the adaptive sample size and sampling interval np control chart", *Quality and Reliability Engineering International*, Vol. 20, No. 6, pp. 553-570.

Xie, M., Goh, T. N., and Kuralmani, V., (2012). "Statistical models and control charts for high-quality processes", Springer Science & Business Media.

Zhang, M., Nie, G., and He, Z., (2014). "Performance of cumulative count of conforming chart of variable sampling intervals with estimated control limits", *International Journal of Production Economics*, Vol. 150, pp. 114-124.

Zhang, Y., Castagliola, P., Wu, Z., and Khoo, M. B., (2012). "The variable sampling interval X chart with estimated parameters", *Quality and Reliability Engineering International*, Vol. 28, No. 1, pp. 19-34.

Zhou, W., Wan, Q., Zheng, Y., and Zhou, Y.-w., (2016). "A joint-adaptive np control chart with multiple dependent state sampling scheme", Communications in Statistics-Theory and Methods (accepted manuscript).